

Structural, Magnetic, and Mössbauer Spectral Study of the Electronic Spin-State Transition in $[\text{Fe}\{\text{HC}(3\text{-Mepz})_2(5\text{-Mepz})\}_2](\text{BF}_4)_2$

Daniel L. Reger,^{*,†} J. Derek Elgin,^{†,‡} Elizabeth A. Foley,[†] Mark D. Smith,[†] Fernande Grandjean,[§] and Gary J. Long^{*,||}

[†]*Department of Chemistry and Biochemistry, University of South Carolina, Columbia, South Carolina 29208,*

[‡]*Department of Chemistry and Physics, Coastal Carolina University, Conway, South Carolina 29528,*

[§]*Department of Physics, B5, University of Liège, B-4000 Sart-Tilman, Belgium, and* ^{||}*Department of Chemistry, Missouri University of Science and Technology, University of Missouri, Rolla, Missouri 65409-0010*

Received June 30, 2009

The complex $[\text{Fe}\{\text{HC}(3\text{-Mepz})_2(5\text{-Mepz})\}_2](\text{BF}_4)_2$ (pz = pyrazolyl ring) has been prepared by the reaction of $\text{HC}(3\text{-Mepz})_2(5\text{-Mepz})$ with $\text{Fe}(\text{BF}_4)_2 \cdot 6\text{H}_2\text{O}$. The solid state structures obtained at 294 and 150 K show a distorted iron(II) octahedral N_6 coordination environment with the largest deviations arising from the restrictions imposed by the chelate rings. At 294 K the complex is predominately high-spin with Fe–N bond distances averaging 2.14 Å, distances that are somewhat shorter than expected for a purely high-spin iron(II) complex because of the presence of an admixture of about 80% high-spin and 20% low-spin iron(II). At 294 K the twisting of the pyrazolyl rings from the ideal C_{3v} symmetry averages only 2.2°, a much smaller twist than has been observed previously in similar complexes. At 150 K the Fe–N bond distances average 1.99 Å, indicative of an almost fully low-spin iron(II) complex; the twist angle is only 1.3°, as expected for a complex with these Fe–N bond distances. The magnetic properties show that the complex undergoes a gradual change from low-spin iron(II) below 85 K to high-spin iron(II) at 400 K. The 4.2 to 60 K Mössbauer spectra correspond to a fully low-spin iron(II) complex but, upon further warming above 85 K, the iron(II) begins to undergo spin-state relaxation between the low- and high-spin forms on the Mössbauer time scale. At 155 and 315 K the complex exhibits spin-state relaxation rates of 0.36 and 7.38 MHz, respectively, and an Arrhenius plot of the logarithm of the relaxation rate yields an activation energy of $670 \pm 40 \text{ cm}^{-1}$ for the spin-state relaxation.

Introduction

Spin-state crossover in iron(II) complexes that contain the FeN_6 coordination environment, first discovered in the 1960s,¹ is important because these complexes have potential applications as optical elements in display devices,^{1,2} as temperature/pressure threshold indicators,² and as “intelligent” contrast agents for biomedical imaging.³ Many of these types of iron(II) complexes are high-spin in the solid state at room temperature and show a cooperative spin-state crossover to the low-spin electronic state upon cooling.¹ Although a number of nitrogen based ligands have been used to prepare a wealth of complexes

that show a spin-state crossover behavior, tris(pyrazolyl)borate complexes, which are of long-term interest to our research programs, were among the first iron(II) complexes studied;⁴ their chemistry is still being developed.⁵

More recently, we⁶ and others⁷ have shown that tris-(pyrazolyl)methane ligands also support unusual spin-state

*To whom correspondence should be addressed. E-mail: reger@mail.chem.sc.edu.

(1) (a) Gütllich, P. In *Mössbauer Spectroscopy Applied to Inorganic Chemistry*; Long, G. J., Ed.; Plenum: New York, 1984; Vol. 1: p. 287. (b) Gütllich, P.; Hauser, A.; Spiering, H. *Angew. Chem., Int. Ed.* **1994**, *33*, 2024.

(2) Kahn, O.; Martinez, C. J. *Science* **1998**, *279*, 44.

(3) Muller, R. N.; Van der Elst, L.; Laurent, S. *J. Am. Chem. Soc.* **2003**, *125*, 8405.

(4) (a) Jesson, J. P.; Trofimenko, S.; Eaton, D. R. *J. Am. Chem. Soc.* **1967**, *89*, 3158. (b) Jesson, J. P.; Weiher, J. F.; Trofimenko, S. *J. Chem. Phys.* **1968**, *48*, 2058. (c) Long, G. J.; Grandjean, F.; Reger, D. L. In *Spin Crossover in Transition Metal Compounds I*; Gütllich, P., Goodwin, H. A., Eds.; Springer: Berlin, 2004; p 91.

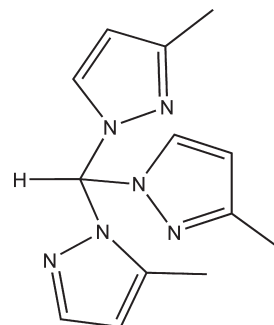
(5) (a) Reger, D. L.; Gardinier, J. R.; Smith, M. D.; Shahin, A. M.; Long, G. J.; Rebbouh, L.; Grandjean, F. *Inorg. Chem.* **2005**, *44*, 1852. (b) Reger, D. L.; Gardinier, J. R.; Gemmill, W.; Smith, M. D.; Shahin, A. M.; Long, G. J.; Rebbouh, L.; Grandjean, F. *J. Am. Chem. Soc.* **2005**, *127*, 2303. (c) Reger, D. L.; Gardinier, J. R.; Elgin, J. D.; Smith, M. D.; Hautot, D.; Long, G. J.; Rebbouh, L.; Grandjean, F. *Inorg. Chem.* **2006**, *45*, 8862. (d) Reger, D. L.; Elgin, J. D.; Smith, M. D.; Grandjean, F.; Rebbouh, L.; Long, G. J. *Polyhedron* **2006**, *25*, 2616.

(6) (a) Reger, D. L.; Little, C. A.; Rheingold, A. L.; Lam, M.; Concolino, T.; Mohan, A.; Long, G. J. *Inorg. Chem.* **2000**, *39*, 4674. (b) Reger, D. L.; Little, C. A.; Rheingold, A. L.; Lam, M.; Liable-Sands, L. M.; Rhagitan, B.; Concolino, T.; Mohan, A.; Long, G. J.; Briois, V.; Grandjean, F. *Inorg. Chem.* **2001**, *40*, 1508. (c) Reger, D. L.; Little, C. A.; Young, V. G., Jr.; Pink, M. *Inorg. Chem.* **2001**, *40*, 2870. (d) Reger, D. L.; Little, C. A.; Smith, M. D.; Long, G. J. *Inorg. Chem.* **2002**, *41*, 4453. (e) Reger, D. L.; Little, C. A.; Smith, M. D.; Rheingold, A. L.; Lam, K.-C.; Concolino, T. L.; Long, G. J.; Hermann, R. P.; Grandjean, F. *Eur. J. Inorg. Chem.* **2002**, 1190. (f) Reger, D. L.; Little, C. A.; Semeniuc, R. F.; Smith, M. D. *Inorg. Chim. Acta* **2009**, *363*, 303. (g) Reger, D. L.; Elgin, J. D.; Smith, M. D.; Grandjean, F.; Rebbouh, L.; Long, G. J. *Eur. J. Inorg. Chem.* **2004**, 3345.

crossover behavior. For example, a combination of X-ray structural, magnetic, and Mössbauer spectral studies have shown that in the solid state $[\text{Fe}\{\text{HC}(3,5\text{-Me}_2\text{pz})_3\}_2](\text{BF}_4)_2$, where pz is a pyrazolyl ring, abruptly changes from fully high-spin iron(II) above 206 K to a 50:50 mixture of high- and low-spin electronic states below 200 K; the spin state composition of this lower temperature mixture does not change as the temperature is lowered to 4.2 K.^{6a-d} This partial changeover occurs even though only one crystallographic iron(II) site is observed at ambient temperature. The spin-state crossover is reversible and shows no hysteresis upon cooling and heating. In this case, we were able to demonstrate that the spin-state crossover behavior was driven by a phase transition that converted the crystallographically equivalent iron(II) sites to two inequivalent sites at low temperature.^{6d} Importantly, as demonstrated by the similar behavior of the $[M\{\text{HC}(3,5\text{-Me}_2\text{pz})_3\}_2](\text{BF}_4)_2$ complexes, where *M* is Co, Ni, and Cu, the phase transition for all four complexes converts half of the sites to a form of the cation in which the twisting of the pyrazolyl rings away from C_{3v} symmetry is very small and converts the other half of the complexes to a form with very large twist angles. Twisting of the rings in poly(pyrazolyl)borate and poly(pyrazolyl)methane complexes favors coordination to larger metal ions,^{5c} such as high-spin iron(II), with typical Fe–N distances of about 2.17 Å, whereas a smaller twist favors smaller metal ions, such as low-spin iron(II), with typical Fe–N bond distances of about 1.98 Å.^{1,5} In $[\text{Fe}\{\text{HC}(3,5\text{-Me}_2\text{pz})_3\}_2](\text{BF}_4)_2$, below the phase transition, all the iron(II) sites with the smaller twist transform to the low-spin state, whereas the iron(II) sites with the larger twist remain high-spin. An important issue, when comparing these results with those previously reported for the tris(pyrazolyl)borate complexes, is that the ionic nature of the complexes apparently prevents loss of crystallinity during the phase transition; in general it appears that the neutral tris(pyrazolyl)borate, FeL_2 complexes shatter when they undergo a phase transition.⁵

Given these interesting results obtained with the $\text{HC}(3,5\text{-Me}_2\text{pz})_3$ ligand, we were interested in preparing additional complexes with analogous, functionalized tris(pyrazolyl)methane ligands. The substitution at the 3-position of a methyl group is necessary to observe spin-state crossover below room temperature because it has been shown that the iron(II) complexes of both tris(pyrazolyl)borate and tris(pyrazolyl)methane ligands without this substitution are low spin at room temperature, changing over to the high-spin state only at higher temperatures.⁴⁻⁶ We specifically wanted to prepare derivatives of $\text{HC}(3\text{-Mepz})_3$ because with $\text{HC}(\text{pz})_3$ we have been able to develop an extensive series of

Chart 1. Drawing of $\text{HC}(3\text{-Mepz})_2(5\text{-Mepz})$



third generation, polytopic ligands, such as $\text{C}_6\text{H}_{6-n}[\text{CH}_2\text{OCH}_2\text{C}(\text{pz})_3]_n$, where *n* is 2, 3, 4, and 6, that link the tris(pyrazolyl)methane units into designed orientations to prepare metal(II) complexes with unique supramolecular coordination network structures.⁸ Building spin-state crossover metal ion centers into these types of networks starting with $\text{HC}(3\text{-Mepz})_3$ might lead to “control” of their properties. Steric considerations involving the methyl groups at the 5-position of $\text{HC}(3,5\text{-Me}_2\text{pz})_3$ prevent such derivative chemistry at the central methine carbon for this ligand.

Unfortunately, it has been shown that attempted preparations of $\text{HC}(3\text{-Mepz})_3$ lead to a mixture of isomers, where the methyl group is located at either the 3- or 5-position of the pz ring, a mixture that does not isomerize to pure $\text{HC}(3\text{-Mepz})_3$.⁹ Fortunately, Pettinari and co-workers⁹ have reported a method for isolating pure $\text{HC}(3\text{-Mepz})_2(5\text{-Mepz})$, shown in Chart 1.

Herein we report the synthesis, the solid-state structures at 150 and 294 K, and the magnetic and Mössbauer spectral properties of $[\text{Fe}\{\text{HC}(3\text{-Mepz})_2(5\text{-Mepz})\}_2](\text{BF}_4)_2$, **1**, a complex that undergoes a spin-state transition with no crystallographic phase transition and shows structural, magnetic, and Mössbauer spectral properties that are consistent with increasing relaxation of the iron(II) between the low-spin and the high-spin electronic states upon warming from about 85 to 400 K.

Experimental Section

General Procedures. All operations were carried out under a nitrogen atmosphere using either standard Schlenk techniques or a drybox. All solvents were dried, degassed, and distilled prior to use. Both $\text{Fe}(\text{BF}_4)_2 \cdot 6\text{H}_2\text{O}$ and 3-methylpyrazole were purchased from Aldrich. The ligand $\text{HC}(3\text{-Mepz})_2(5\text{-Mepz})$ was synthesized according to a literature method.⁹

The magnetic susceptibilities of **1** have been measured in a 0.1 and 2 T applied field with a Quantum Design MPMS XL SQUID magnetometer. Gelatin capsules were used as sample containers for measurements between 5 and 400 K. The very small diamagnetic contribution of these capsules makes a negligible contribution to the overall magnetization, which was dominated by the sample. A diamagnetic correction of -0.000320 emu/mol, obtained from tables of Pascal's constants, has been applied to the measured molar magnetic susceptibility of **1**.

The Mössbauer spectra of **1** have been measured between 4.2 and 315 K on a constant-acceleration spectrometer that utilized a room temperature rhodium matrix cobalt-57 source and was calibrated at 295 K with α -iron powder. The spectra have been measured on an absorber that contained 50 mg/cm² of powder

(7) (a) Anderson, P. A.; Astley, T.; Hitchman, M. A.; Keene, F. R.; Moubaraki, B.; Murray, K. S.; Skelton, B. W.; Tiekink, E. R. T.; Toftlund, H.; White, A. H. *J. Chem. Soc., Dalton Trans.* **2000**, 3505. (b) Paulsen, H.; Dueland, L.; Zimmermann, A.; Averseng, F.; Gerdan, M.; Winnler, H.; Toftlund, H.; Trautwein, A. X. *Monatsh. Chem.* **2003**, 134, 295. (c) Moubaraki, B.; Leita, B. A.; Halder, G. J.; Batten, S. R.; Jensen, P.; Smith, J. P.; Cashion, J. D.; Kepert, C. J.; Létard, J.-F.; Murray, K. S. *J. Chem. Soc., Dalton Trans.* **2007**, 4413.

(8) (a) Reger, D. L.; Gardinier, J. R.; Semeniuc, R. F.; Smith, M. D. *J. Chem. Soc., Dalton Trans.* **2003**, 1712. (b) Reger, D. L.; Wright, T. D.; Semeniuc, R. F.; Grattan, T. C.; Smith, M. D. *Inorg. Chem.* **2001**, 40, 6212. (c) Reger, D. L.; Semeniuc, R. F.; Smith, M. D. *Eur. J. Inorg. Chem.* **2002**, 543. (d) Reger, D. L.; Semeniuc, R. F.; Smith, M. D. *J. Chem. Soc., Dalton Trans.* **2002**, 476. (e) Reger, D. L.; Semeniuc, R. F.; Smith, M. D. *J. Organomet. Chem.* **2003**, 666, 87. (f) Reger, D. L.; Semeniuc, R. F.; Silaghi-Dumitrescu, I.; Smith, M. D. *Inorg. Chem.* **2003**, 42, 3751. (g) Reger, D. L.; Semeniuc, R. F.; Smith, M. D. *Inorg. Chem.* **2003**, 42, 8137.

(9) Pettinari, C.; Pellei, M.; Cingolani, A.; Martini, D.; Drozdov, A.; Troyanov, S.; Panzeri, W.; Mele, A. *Inorg. Chem.* **1999**, 38, 5777.

Table 1. Crystallographic Data for the Structural Analyses of **1**

parameter	294 K	150 K
formula	C ₂₆ H ₃₂ B ₂ F ₈ FeN ₁₂	C ₂₆ H ₃₂ B ₂ F ₈ FeN ₁₂
formula weight, g/mol	742.11	742.11
space group	<i>P</i> 2 ₁ / <i>c</i>	<i>P</i> 2 ₁ / <i>c</i>
<i>a</i> , Å	9.6583(5)	9.6343(5)
<i>b</i> , Å	13.1965(7)	13.0290(6)
<i>c</i> , Å	13.9799(7)	13.5476(6)
α , deg	90	90
β , deg	107.8800(10)	108.3360(10)
γ , deg	90	90
<i>V</i> , Å ³	1695.76(15)	1614.22(13)
<i>Z</i>	2	2
crystal color	pale pink	purple
ρ (calcd), Mg/m ³	1.453	1.527
<i>R</i> (<i>F</i>) ^a , (<i>wF</i> ²) ^a	0.0782, 0.2278	0.0485, 0.1293

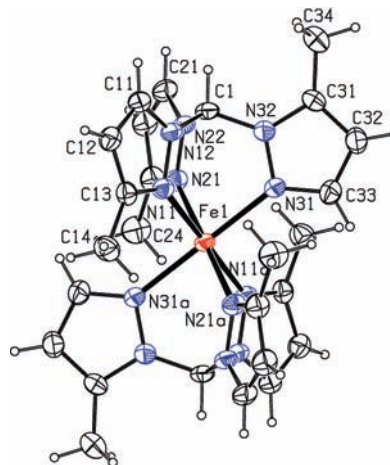
^aQuantity minimized = $R(wF^2) = [\sum w(F_o^2 - F_c^2)^2 / \sum w(F_o^2)^2]^{1/2}$; $R = \sum \Delta / \sum |F_o|$, $\Delta = |F_o| - |F_c|$.

that had been crushed but not ground and dispersed in boron nitride powder. The spectra obtained at 4.2 to 60 K have been fit with a single low-spin iron(II) quadrupole doublet with relative statistical errors of ± 0.005 mm/s for the isomer shifts, ± 0.01 mm/s for the quadrupole splittings, and ± 0.005 (% ϵ)(mm/s) for the spectral absorption areas. The spectra obtained between 85 and 315 K have been fit with a relaxation profile as discussed below and relative statistical errors are ± 0.01 mm/s for the isomer shifts, ± 0.02 mm/s for the quadrupole splittings, ± 0.2 MHz for the relaxation rate, and ± 0.01 (% ϵ)(mm/s) for the spectral absorption areas; in both cases the absolute errors are estimated to be approximately twice as large.

Synthesis of [Fe{HC(3-Mepz)₂(5-Mepz)}₂](BF₄)₂, **1.** A 50 mL round-bottom flask was charged with bis(3-methyl-1-pyrazolyl)(5-methyl-1-pyrazolyl)methane (0.25 g, 1.0 mmol) and 15 mL of tetrahydrofuran (thf). A second 50 mL round-bottom flask was charged with Fe(BF₄)₂·6H₂O (0.165 g, 0.50 mmol) and 10 mL of thf. Once the materials were dissolved, the ligand solution was added via cannula transfer to the flask containing the Fe(BF₄)₂·6H₂O. The mixture was stirred for 6 h, during which time a copious precipitate had formed. The solvent was removed via cannula filtration, and the precipitate was dried under vacuum overnight. The reaction yielded 0.279 g of **1** (77% yield). X-ray quality crystals were grown by layering an acetone solution of **1** with hexanes. Anal. Calcd for C₂₆H₃₂B₂F₈FeN₁₂: C, 42.08; H, 4.35; N, 22.65; Found: C, 41.93; H, 3.98; N, 22.25. HRMS: ESI(+) (*m/z*) calcd for [C₂₆H₃₂N₁₂Fe¹⁰BF₄]⁺ 654.2291, found 654.2294. MS ESI(+) (*m/z*) (rel. % abund.) [assgn]: 655 (4) [C₂₆H₃₂N₁₂FeBF₄]⁺, 284 (100) [C₂₆H₃₂N₁₂Fe]²⁺.

X-ray Structural Data. The X-ray crystallographic data for [Fe{HC(3-Mepz)₂(5-Mepz)}₂](BF₄)₂ are given in Table 1. Evaluation of crystal quality, unit cell determinations and X-ray intensity data measurements were performed using a Bruker SMART APEX CCD-based diffractometer and 0.71073 Å Mo K α radiation.¹⁰ Two data sets were collected on the same crystal at 294 and 150 K. Raw data frame integration and *Lp* corrections were performed with SAINT+.¹⁰ Final unit cell parameters were determined by least-squares refinement of all reflections with $I > 5\sigma(I)$ from each data set. Absorption corrections were not applied. Direct methods structure solution of the 294 K structure, difference Fourier calculations, and full-matrix least-squares refinement against *F*² were performed with SHELXTL.¹¹

High Temperature Structure. At 294 K the crystal is pale pink. Systematic absences in the intensity data were consistent with the space group *P*2₁/*c*. The asymmetric unit contains half of the

**Figure 1.** Structure of the cation in [Fe{HC(3-Mepz)₂(5-Mepz)}₂](BF₄)₂, **1**, obtained at 294 K.

[Fe{HC(3-Mepz)₂(5-Mepz)}₂]²⁺ cation on a crystallographic inversion center, and a severely disordered BF₄⁻ counterion. The BF₄⁻ was modeled as adopting three distinct orientations, with fixed occupancies 0.45/0.40/0.15. A total of 45 B–F and F–F distance restraints were applied to maintain a chemically reasonable geometry for each disordered component. The boron ion was assigned a common anisotropic displacement parameter; all F⁻ ions were assigned a common isotropic displacement parameter. After the final refinement, the presence of the several residual electron peaks with < 1 e⁻/Å³ in the disordered region indicates the limitations of the 3-fold disorder model. With the noted exceptions, all non-hydrogen atoms were refined with anisotropic displacement parameters. Hydrogen atoms were placed in geometrically idealized positions and included as riding atoms.

Low Temperature Structure. After obtaining the 294 K data, the same crystal was cooled slowly, in 10 K increments. Cooling is accompanied by a gradual deepening of the room-temperature pale pink hue such that, at about 200 K, the crystal is deep purple. There is no change in the *P*2₁/*c* space group upon cooling to 150 K, but the expected about 4.8% contraction of the unit cell volume is observed; the asymmetric unit is the same at 150 and 294 K. Refinement of the 150 K data converged rapidly using the structural model obtained at 294 K. The BF₄⁻ disorder is not appreciably affected at the lower temperature, and the disorder was treated similarly, with the exception that the major disorder components were refined anisotropically. The minor component of the BF₄⁻ is still isotropic.

Results

Structural Studies. The [Fe{HC(3-Mepz)₂(5-Mepz)}₂](BF₄)₂, **1**, complex has been prepared by the reaction of HC(3-Mepz)₂(5-Mepz) with Fe(BF₄)₂·6H₂O, and crystals were grown by layering an acetone solution with hexanes. The solid state structure of **1** has been determined at both 294 and 150 K. At 294 K the crystals have a pale pink color indicating that a small population of the low spin form is present, an observation that has been verified by magnetic and Mössbauer spectral studies, vide infra. Typically, high-spin iron(II) pyrazolyl complexes of this type are colorless, whereas low-spin complexes are purple.^{4–6}

Figure 1 shows the 294 K structure and numbering scheme of the cation in **1**, and Table 2 gives important bond distances and angles. The N₆ coordination environment is a distorted octahedron, with the largest deviations

(10) SMART Version 5.625 and SAINT+ Version 6.22; Bruker Analytical X-ray Systems, Inc.: Madison, WI, 2001.

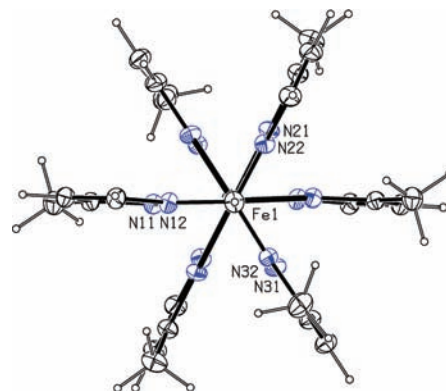
(11) Sheldrick, G. M. SHELXTL, Version 6.1; Bruker Analytical X-ray Systems, Inc.: Madison, WI, 2000.

Table 2. Selected Bond Distances and Angles for **1**

temperature	294 K	150 K
Bond Distances (Å)		
Fe–N(11)	2.163(4)	1.998(3)
Fe–N(21)	2.153(4)	2.002(3)
Fe–N(31)	2.118(4)	1.978(3)
C(1)–N(12)	1.442(6)	1.439(4)
C(1)–N(22)	1.442(7)	1.443(4)
C(1)–N(32)	1.436(6)	1.441(4)
Bond Angles (deg)		
N(11)–Fe–N(21)	84.14(17)	87.05(10)
N(11)–Fe–N(31)	84.99(17)	88.14(10)
N(21)–Fe–N(31)	85.01(16)	88.31(10)
N(11)–Fe–N(11a)	180	180
N(11)–Fe–N(21a)	95.86(17)	92.95(10)
N(11)–Fe–N(31a)	95.01(17)	91.86(10)
N(21)–Fe–N(31a)	94.99(16)	91.69(10)
N(12)–C(1)–N(22)	110.5(4)	109.4(3)
N(12)–C(1)–N(32)	111.9(4)	110.4(3)
N(22)–C(1)–N(32)	111.4(4)	110.5(3)
FeN(11)–N(12)C(1) torsion	2.0(5)	0.7(3)
FeN(21)–N(22)C(1) torsion	3.2(5)	3.1(3)
FeN(31)–N(32)C(1) torsion	1.5(6)	0.9(4)

arising from the restrictions imposed by the chelate rings with intraligand N–Fe–N angles averaging 84.7°. The Fe–N bond distances range from 2.118(4) to 2.163(4) Å with an average of 2.14 Å. These distances are slightly shorter than expected for a fully high-spin complex of this type; in [Fe{HC(3,5-Me₂pz)₃}₂](BF₄)₂ they average 2.17 Å at the same temperature.^{6b} These shorter distances are a result of the presence of an admixture of the low-spin and high-spin iron(II) states at 294 K because the average low-spin Fe–N distance is 1.99 Å in the fully low-spin complex, as is discussed below. The iron(II) U_{iso} values, herein derived from the anisotropic values and thus actually U_{eq} values, of 0.0331(2) and 0.0542(4) Å², obtained at 150 and 294 K, respectively (i.e., the “thermal ellipsoids”), are both somewhat larger than expected as a result of the superimposition at the same site of an admixture of the low-spin and high-spin forms of the complex. The substantial increase in the thermal parameters of **1** in comparison with those of the more normal [Fe{HC(3,5-Me₂pz)₃}₂](BF₄)₂ complex^{6a,c} is shown in Supporting Information, Figure S1; the significance of this increase in the analysis of the Mössbauer spectral results is discussed below.

As we have noted previously,^{5,6} an important parameter that has a significant effect on the spin-state cross-over behavior of these types of complexes is the “twist” the pyrazolyl rings make away from ideal C_{3v} symmetry. In the absence of twisting, the iron(II) ion is in the plane of the pyrazolyl rings and the FeN(n1)–N(n2)C(methine) torsion angles are 0°. In both poly(pyrazolyl)borate complexes, where the torsion angle is MN(n1)–N(n2)B, and in poly(pyrazolyl)methane metal(II) complexes, this torsion angle increases as the size of the metal(II) ion increases because the bite angle of these ligands is largely fixed and increasing the twisting allows the ligands to bond to larger metal ions.⁶ In the high-spin structures⁶ of [Fe{HC(3,5-Me₂pz)₃}₂]²⁺ with different counterions and solvents this torsion angle averages 11.7°, with a range of 9.8 to 13.1°; in contrast, for **1** the torsion angles average

**Figure 2.** View of the cation in the 294 K structure of **1** down its approximate C_{3v} axis.

2.2°. Although this angle in **1** is reduced by the presence of a small portion of the low-spin iron(II) state, whose torsion angle averages 1.3° at 150 K, *vide infra*, the twist is very small for a high-spin iron(II) complex.^{5c} A view down the approximate C_{3v} axis, see Figure 2, shows the lack of any significant distortion for this cation at 294 K.

Slow cooling of the same crystal used for the 294 K study to 150 K leads to a color change from pale pink to deep purple, a change that is indicative of a mainly low-spin iron(II) state for **1** at 150 K, a change that is confirmed by the magnetic and Mössbauer spectral studies, *vide infra*. No phase transition is observed upon cooling; the numbering scheme is the same as shown for the 294 K structure in Figure 1, and Table 2 shows important bond distances and angles obtained at 150 K. The basic octahedral geometry remains with average intraligand N–Fe–N angles averaging 87.8°. The average 1.99 Å Fe–N bond distances clearly indicate that the iron(II) is in the predominantly low-spin state.⁴ The FeN(n1)–N(n2)C(methine) torsion angles average 1.3°, an angle that is typical of low-spin complexes of this type.⁶

Magnetic Results. The temperature dependence of the molar magnetic susceptibility, χ_M , of [Fe{HC(3-Mepz)₂(5-Mepz)₂}(BF₄)₂], **1**, has been measured after zero-field cooling to 5 K followed by warming to 400 K and subsequent cooling in a 0.1 T applied field; a second cycle of heating and cooling yielded virtually identical results. Further, as would be expected for a paramagnetic complex, virtually identical results have been obtained between 5 and 300 K in a 2 T applied field.

The temperature dependencies of $\chi_M T$ and $1/\chi_M$ are shown in Figure 3a, and the temperature dependence of χ_M and the corresponding effective magnetic moment, μ_{eff} , are shown in the Supporting Information, Figures S2 and S3. The 400 K μ_{eff} is 4.90 μ_B , a moment that is equal to the spin-only moment expected for a high-spin iron(II) complex with a nominal octahedral ⁵T_{2g} electronic ground state.^{4,12} At lower temperatures, **1** exhibits a gradual decrease in χ_M , $\chi_M T$, and μ_{eff} such that at 100 K and below the complex has a rather small moment as would be expected of a low-spin iron(II) complex with a nominal octahedral ¹A_{1g} electronic ground state. These gradual decreases are typical of an iron(II) electronic spin-state transition and, as expected, the transition is

(12) Figgis, B. N. *Introduction to Ligand Fields*; Wiley-Interscience: New York, 1966; p 274.

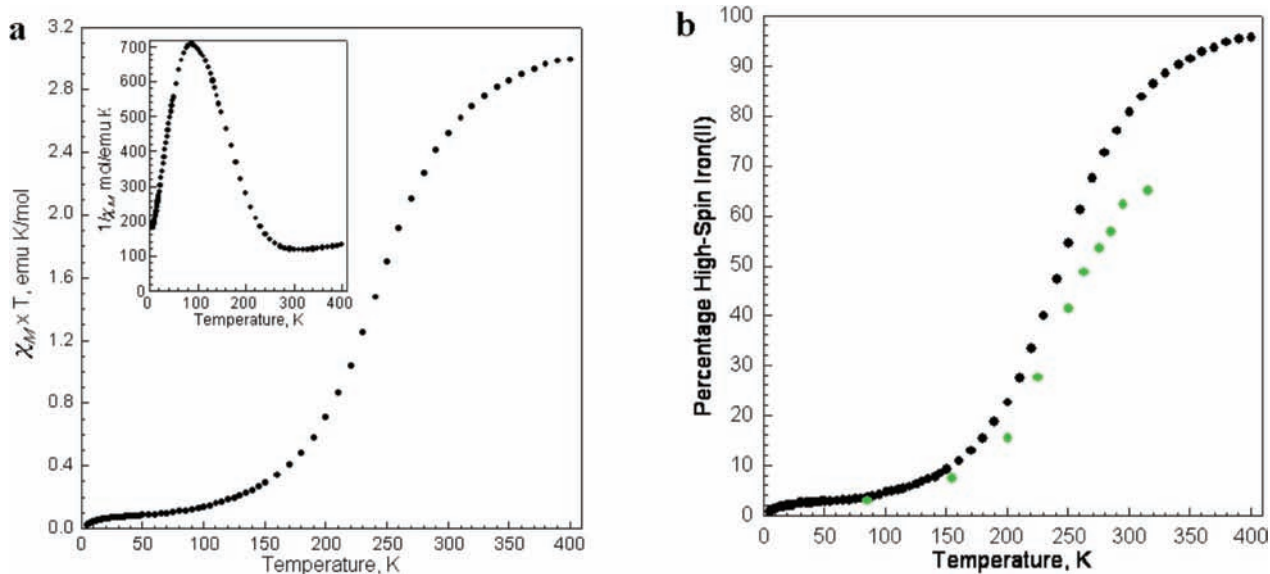


Figure 3. (a) Temperature dependence of $\chi_M T$ and $1/\chi_M$, inset, obtained for **1** after zero-field cooling and subsequent warming and cooling in a 0.1 T applied field. (b) The temperature dependence of the percentage of high-spin iron(II) present in **1**, the black points. The green points correspond to the percentages obtained from the Mössbauer spectral relaxation fits in the absence of any difference between the low-spin and high-spin iron(II) recoil-free fractions, f .

much more gradual than is generally observed for a cooperative iron(II) spin-state crossover in these types of complexes.⁶

The temperature dependence of the transition from the low-spin iron(II) state at lower temperatures to the high-spin iron(II) state at higher temperatures, see Figure 3b, has been obtained with the assumption that the low-spin iron(II) state in **1** has a temperature independent molar magnetic susceptibility equivalent to $0.1 \mu_B$ at 300 K, a typical second-order Zeeman contribution to the susceptibility in low-spin iron(II) complexes. Further, it has been assumed that the high-spin iron(II) state in **1** has a moment of $5.0 \mu_B$, a moment that is between the spin-only moment of $4.90 \mu_B$ and the $5.2 \mu_B$ moment often observed in distorted high-spin iron(II) complexes at 295 K. As may be observed in Figure 3b, the spin-state transition occurs predominately between 150 and 350 K, a temperature range that is larger than is often observed for such transitions. The choice of 0.1 and $5.0 \mu_B$ for the two states is a bit arbitrary, but these values give the most reasonable and consistent variation in the spin-state population. The results obtained with alternative limiting moments, see Supporting Information, Figure S4, are quite similar and lead to the same basic results.

Mössbauer Spectral Properties. The Mössbauer spectra of **1** have been measured between 4.2 and 315 K, and some of the resulting spectra are shown in Figure 4. The 4.2, 30, and 60 K spectra of **1** reveal the presence of only a low-spin iron(II) quadrupole doublet with line widths of 0.28, 0.29, and 0.30 mm/s, respectively; the low-spin iron(II) hyperfine parameters are given in Table 3A. With increasing temperature, at 85 K and above, a second quadrupole doublet, characteristic of high-spin iron(II), appears and gradually increases in relative area, but with much larger line widths for both the high-spin and low-spin iron(II) doublets. These changes with increasing temperature are a signature of a complex that is undergoing electronic spin-state relaxation on the Mössbauer time scale of 10^{-8} s. As a

consequence, the spectra of **1** have been fit with an electronic spin-state relaxation profile based on the approach of Litterst and Amthauer.¹³

In the relaxation fits the observed spectral line profile¹³ depends upon the relaxation rate, λ , the percentage population of the high-spin state, p , and the low-spin state, $100 - p$, and the hyperfine parameters of the high-spin and low-spin iron(II) electronic states. This model assumes that the high-spin and low-spin iron(II) states have an equivalent recoil-free fraction, f , at a given temperature, an assumption that may or may not be acceptable, but that is often used. As shown in Figure 4, the relaxation rate and the population, p , of the high-spin state, as well as the isomer shifts and quadrupole splittings of both the high-spin and low-spin states, have been fit, and the resulting parameters are given in Tables 3A and 3B. In all the fits, the line width has been constrained at 0.30 mm/s, which is the line width observed at 60 and 85 K for the low-spin doublet.

Acceptable relaxation fits required different signs for the electric field gradients of the two spin-states, and the high-spin state has tentatively been taken to be negative on the basis of recent calculations¹⁴ on related complexes; relaxation fits with the same sign for both spin-states were unsuccessful. A similar requirement for different signs has been observed earlier^{5b} for several related complexes undergoing a similar spin-state relaxation.

The temperature dependence of the isomer shifts and quadrupole splittings of **1**, resulting from the relaxation fits, is shown in Figure 5. In all cases the parameters are typical of the high-spin and low-spin iron(II) ions in pyrazolyl ligand-based complexes. The temperature dependence of the high-spin iron(II) isomer shift behaves exactly as would be expected from the structure of **1**. A fit of this temperature dependence with the Debye model for a solid yields a Mössbauer temperature, Θ_M , of 170 ± 30 K,

(13) Litterst, F. J.; Amthauer, G. *Phys. Chem. Miner.* **1984**, *10*, 250.

(14) Remacle, F.; Grandjean, F.; Long, G. J. *Inorg. Chem.* **2008**, *47*, 4005.

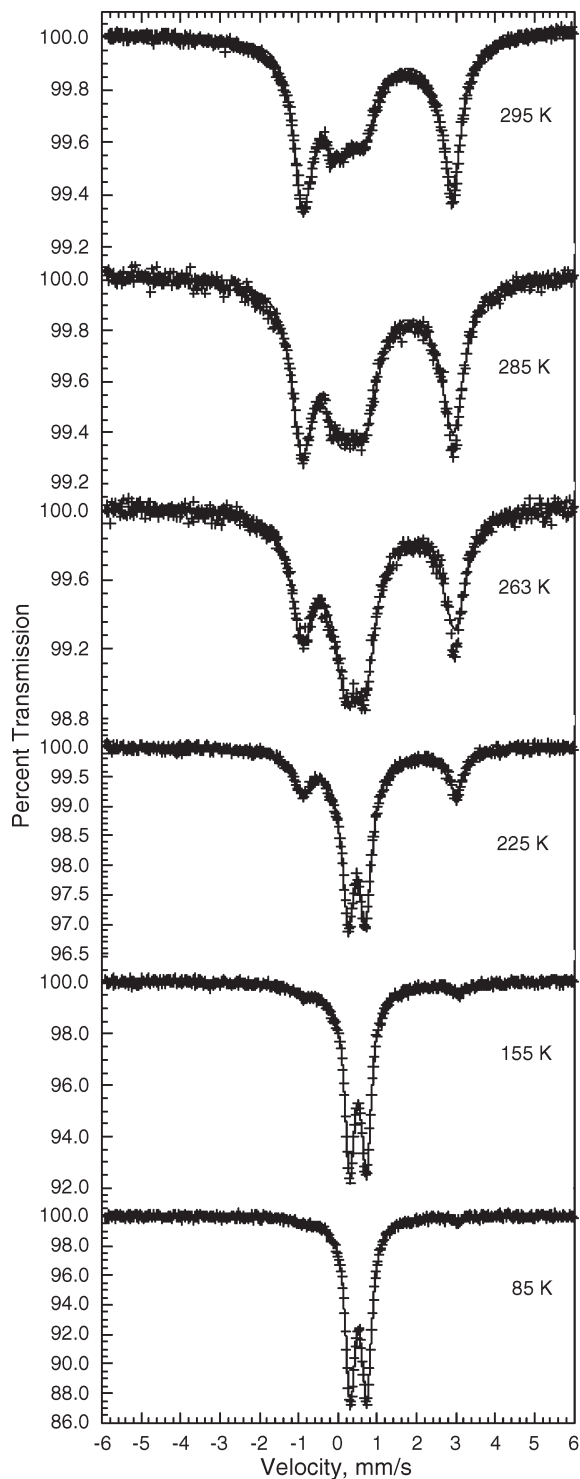


Figure 4. Mössbauer spectra of **1** obtained at the indicated temperatures and fit with a single relaxation profile. In most cases the line corresponding to the fit is obscured by the data points.

a rather small value that is consistent with the unusually large thermal factor observed for **1** at 295 K, see below. Further, the high-spin iron(II) is in a coordination environment at 295 and 315 K that is essentially an admixture of the high-spin and a low-spin iron(II) states.

In contrast, the isomer shift of the low-spin iron(II) decreases between 4.2 and 263 K with a Θ_M of 709 ± 17 K, a value that is rather large but not unexpected for low-spin iron(II). However, above 263 K the low-spin iron(II)

isomer shift decreases slightly presumably because of changes in the low-spin iron(II) coordination environment. A concomitant increase in the magnitude of the low-spin iron(II) quadrupole splitting occurs above about 263 K. The quadrupole splitting of the low-spin state is determined by the lattice contribution to the electric field gradient, a contribution that seemingly increases as the population of the high-spin state increases. In contrast, the quadrupole splitting of the high-spin iron(II), which is rather large in magnitude at about -3.9 mm/s, is virtually independent of temperature. The high-spin iron(II) quadrupole splitting is dominated by a valence contribution to the electric field gradient, and the lack of any temperature dependence indicates that any splitting of the high-spin iron(II) t_{2g} orbitals by the low-symmetry component of the pseudooctahedral crystal field must be large enough to prevent any significant change in the relative population of these orbitals¹⁵ between 85 and 315 K.

An Arrhenius plot of the logarithm of the relaxation rate, λ , obtained between 85 and 315 K for **1** is shown in Figure 6. The resulting linear Arrhenius plot yields an activation energy for the electronic spin-state relaxation of 670 ± 40 cm⁻¹, a value which is somewhat smaller than is typical of such relaxation processes, such as the activation energy of 1760 cm⁻¹ observed¹⁶ for the related molecular Fe[HB(pz)₃]₂ complex; it is also much smaller than the 2820 cm⁻¹ observed^{5b} for the ionic [Fe{HC(pz)₃]₂(BF₄)₂ complex. The corresponding temperature dependence of the percentage of the high-spin iron(II) population obtained for the relaxation is shown in the inset to Figure 6. The increase in the high-spin iron(II) population is in qualitative but not quantitative agreement with the percentage of high-spin iron(II) determined from the magnetic properties of **1**, see Figure 3b. The most possible reason for the increasing difference with increasing temperature is presented in the Discussion section.

The temperature dependence between 4.2 and 225 K of the logarithm of the total Mössbauer spectral absorption area of **1**, see Figure 7, is well fit with the Debye model^{6a,c,17} for a solid and yields a Debye temperature, Θ_D , of 139(2) K. Above 225 K, the measured absorption areas and their logarithms are substantially smaller than expected from the temperature dependence between 4.2 and 225 K, as a result of the spin-state transition and the increasing percentage of high-spin iron(II) ions. The solid line in Figure 7 may be interpreted as the temperature dependence of the low-spin iron(II) f -factor, whereas the data obtained above 225 K reflect the decrease in the f -factor as a result of an increasing percentage of the high-spin iron(II) state.

It is well-known¹⁷ that the two temperatures, Θ_M and Θ_D obtained from the temperature dependencies of the isomer shift and of the logarithm of the absorption area, are usually different because they depend on $\langle v^2 \rangle$ and $\langle x^2 \rangle$, respectively, where $\langle v^2 \rangle$ is the mean-square vibrational velocity of the iron-57 nuclide and $\langle x^2 \rangle$ is the mean-square displacement of the iron-57 nuclide; unfortunately, there

(15) Ingalls, R. *Phys. Rev.* **1964**, *133*, A787.

(16) Grandjean, F.; Long, G. J.; Hutchinson, B. B.; Ohlhausen, L.; Neill, P.; Holcomb, J. D. *Inorg. Chem.* **1989**, *28*, 4406.

(17) Shenoy, G. K.; Wagner, F. E.; Kalvius, G. M. In *Mössbauer Isomer Shifts*; Shenoy, G. K.; Wagner, F. E., Eds.; Elsevier Science: North-Holland, Amsterdam, 1978; p 49.

Table 3A. Mössbauer Spectral Hyperfine Parameters for **1**

T, K	δ_{HS} , mm/s ^a	δ_{LS} , mm/s ^a	$\Delta E_{\text{Q,HS}}$, mm/s	$\Delta E_{\text{Q,LS}}$, mm/s	total area, (% ϵ)(mm/s)
315	0.964	0.337	-3.89	0.91	1.69
295	0.986	0.366	-3.91	0.85	2.14
285	0.987	0.403	-3.96	0.78	2.41
275	1.006	0.434	-3.98	0.67	2.68
263	1.015	0.457	-3.98	0.61	2.99
250	1.030	0.468	-4.00	0.53	3.43
225	1.042	0.482	-3.96	0.47	4.48
200	1.063	0.498	-3.97	0.44	5.73
155	1.085	0.507	-3.89	0.43	7.55
85	1.130	0.519	-3.82	0.42	11.59
60		0.521		0.41	14.16
30		0.524		0.41	16.65
4.2		0.523		0.41	18.16

^a The isomer shifts are given relative to 295 K α -iron powder.

Table 3B. Mössbauer Spectral Relaxation Parameters for **1**

T, K	λ , mm/s	λ , MHz	$\ln \lambda$	p , %
315	0.636	7.38	2.00	65.1
295	0.563	6.54	1.88	62.3
285	0.543	6.30	1.84	56.9
275	0.493	5.72	1.74	53.5
263	0.411	4.77	1.56	48.9
250	0.313	3.63	1.29	41.4
225	0.202	2.35	0.854	27.7
200	0.112	1.30	0.263	15.5
155	0.031	0.360	-1.02	7.5
85	0.00018	0.0021	-6.17	3.0

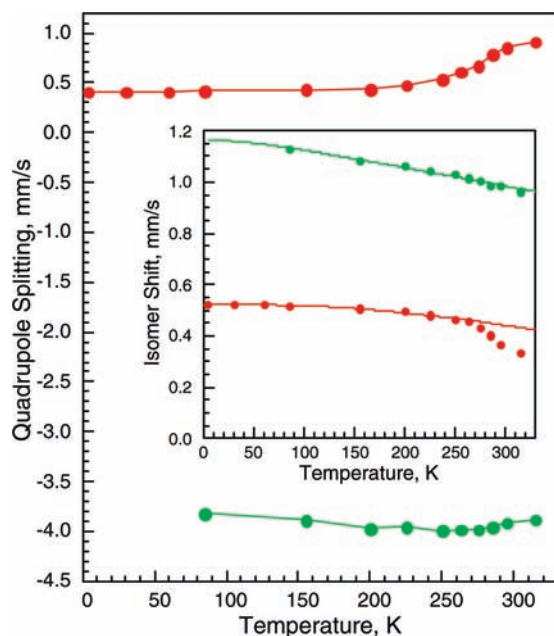


Figure 5. Temperature dependence of the isomer shift of the high-spin, green, and the low-spin, red, iron(II), inset, and the corresponding quadrupole splitting of **1** as obtained from the relaxation fits. The error bars are no larger than the data points. In the inset the solid lines correspond to a fit with the Debye model for a solid between 85 and 315 K for the high-spin iron(II) and between 4.2 and 263 K for the low-spin iron(II).

is no model independent relationship¹⁷ between these mean-square values. However, the values at these temperatures reported¹⁸ for other iron(II) complexes indicate

(18) Owen, T.; Grandjean, F.; Long, G. J.; Domasevitch, K. V.; Gerasimchuk, N. *Inorg. Chem.* **2008**, *47*, 8704.

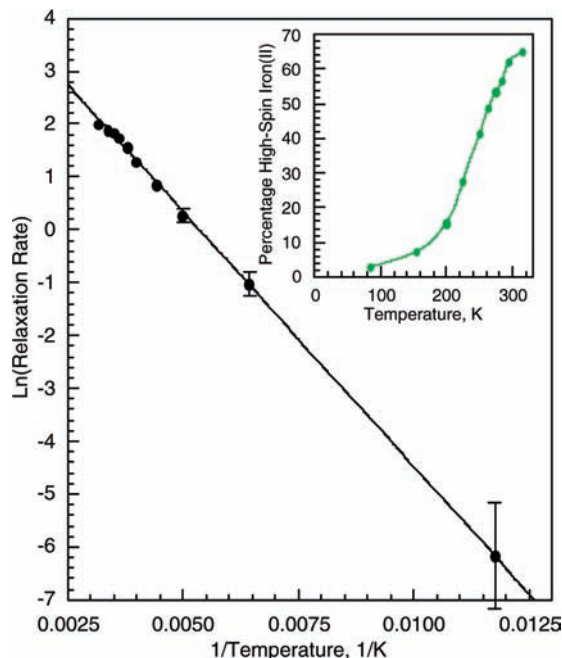


Figure 6. Arrhenius plot of the logarithm of the relaxation rate obtained for **1** between 85 and 315 K. Unless error bars are shown the errors are no larger than the size of the data points. Inset: The percentage of the high-spin iron(II) electronic spin-state of **1** as a function of temperature.

that Θ_{M} , which is more sensitive to the high-frequency phonons, is often two to four times larger than Θ_{D} . In **1**, the Θ_{D} of 139(2) K is small as a result of the large iron(II) U_{iso} values of 0.0331 and 0.0542 \AA^2 and the correspondingly small f -factors of 0.170 and 0.055 obtained at 150 and 294 K, respectively, for the iron(II) ions. This Θ_{D} value is similar to the Θ_{M} value of 170(30) K observed for the high-spin iron(II), but substantially smaller than the 720(20) K value observed for the low-spin iron(II).

A careful inspection of Figure 4 reveals that there is some misfit, especially at about 3 mm/s in the fits of the Mössbauer spectra of **1** at 263 to 295 K, a misfit that probably results from the use of a single relaxation rate in the fits shown in Figure 4. This misfit cannot be avoided by using a smaller line width in these fits. As a consequence, we have fit the 295 K spectrum with two relaxation rates to represent what may well be a small distribution of relaxation rates. The resulting fit, see Figure 8, avoids this misfit and yields relaxation rates of 4.44 and 17.6 MHz and high-spin percentages, p , of 67 and 54% for the two relaxation components, values which, as expected, bracket the value found for the single relaxation component fit. This fit indicated that there is probably a small distribution of the relaxation rates but that the values given in Table 3B represent a good average value.

Discussion

Although the complex $[\text{Fe}\{\text{HC}(3\text{-Mepz})_2(5\text{-Mepz})\}_2](\text{BF}_4)_2$, **1**, is rather similar to the $[\text{Fe}\{\text{HC}(3,5\text{-Me}_2\text{pz})_3\}_2](\text{BF}_4)_2$,^{6a-d} $[\text{Fe}\{\text{HC}(3,5\text{-Me}_2\text{pz})_3\}_2]\text{I}_2$,^{6c} and $[\text{Fe}\{\text{HC}(3,4,5\text{-Me}_3\text{pz})_3\}_2](\text{BF}_4)_2$ ^{6g} complexes we have studied previously, its behavior is unique in a number of respects. The X-ray structural, magnetic, and Mössbauer spectral studies of **1** have shown the presence of an admixture of the low-spin and

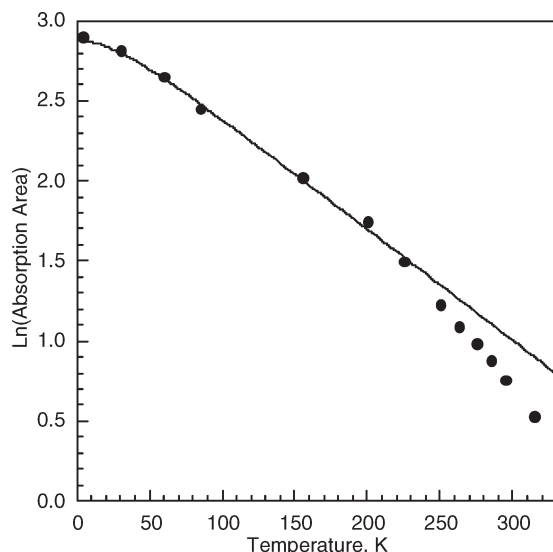


Figure 7. Temperature dependence of the logarithm of the Mössbauer spectral absorption area of **1**. The solid line corresponds to a fit with the Debye model for a solid for the data obtained between 4.2 and 225 K.

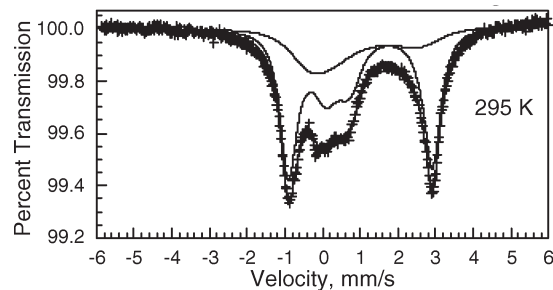


Figure 8. Mössbauer spectra of **1** obtained at 295 K and fit with two relaxation profiles.

Table 4. Average Pyrazolyl Ring Torsion Angles in High-Spin Iron(II) Tris(pyrazolyl)methane Complexes

complex	average FeN(n1)–N(n2)C (methine) torsion angle, deg
[Fe{HC(3,5-Me ₂ pz) ₃ } ₂](BF ₄) ₂	11.7
[Fe{HC(3,5-Me ₂ pz) ₃ } ₂]I ₂	8.7
[Fe{HC(3,5-Me ₂ pz) ₃ } ₂]I ₂ ·(CH ₂ Cl ₂) ₄	17.7
[Fe{HC(3,4,5-Me ₃ pz) ₃ } ₂](BF ₄) ₂	5.1
[Fe{HC(3-Mepz) ₂ (5-Mepz)} ₂](BF ₄) ₂ , 1	2.2

high-spin iron(II) states at temperatures from 85 to 400 K, an admixture that gradually shifts from predominately low-spin to predominately high-spin with increasing temperature. In contrast, both [Fe{HC(3,5-Me₂pz)₃}₂](BF₄)₂^{6b} and [Fe{HC(3,4,5-Me₂pz)₃}₂](BF₄)₂^{6g} are fully high-spin at temperatures above 200 and 110 K, respectively, and the spin-state change upon cooling below these temperatures is an abrupt, cooperative spin-state crossover. Interestingly, as proven by X-ray crystallography for the former and indicated by the shattering of the crystals at the spin-crossover temperature for the latter, both of these complexes undergo a phase transition at the spin-crossover temperature. In contrast, complex **1** does *not* undergo a phase transition between 150 and 294 K, as shown herein. This difference supports our previous arguments with analogous poly(pyrazolyl)borate complexes and extends to poly(pyrazolyl)methane complexes the contention that phase transitions, when present, dominate the

spin-crossover behavior of this class of complexes; such phase transitions are often absent in the case of a gradual spin-state transition as is observed for **1**.^{5a,b}

An explanation for the different spin-state behavior of **1** is derived from the solid state structure of the predominately high-spin complex obtained at 294 K. In nearly all of the structures of the high-spin FeL₂ complexes with the poly(pyrazolyl)borate and [FeL₂]²⁺ cations with poly(pyrazolyl)methane ligands that we and others have reported, the pyrazolyl rings are twisted; see Table 5 in reference 5c and Table 4. This twist angle is small for the low-spin forms of these complexes.⁶ During the spin-state conversion, both the Fe–N bond distances and twist angles must change. For **1** with the lowest twist angle in the table, only modest reorganization is needed during the spin-state change; *there is no need for the substantial cooperative effects* associated with abrupt spin-state crossover behavior.

Two examples^{5b,d} from the more extensively studied poly(pyrazolyl)borate complexes indicate the correlation of the ring twisting with spin crossover behavior. The Fe[(*p*-HC₂-C₆H₄)B(3-Mepz)₃]₂ complex has two crystallographically independent iron(II) molecules, one with an FeN–NB torsion angle of 9.2° at 294 K that undergoes a spin-state crossover at 110 K, whereas the other has a smaller FeN–NB torsion angle of 6.0° at 294 K and undergoes a gradual spin-state transition between 200 and 300 K.^{5b} Another example is the similar Fe[(C₆H₅)B(3-Mepz)₃]₂ complex in which the average torsion angle is 12.0° and does not undergo a spin-crossover to the low-spin state above 4 K.^{5d} In poly(pyrazolyl)methane chemistry, the non-solvated crystalline form of [Fe{HC(3,5-Me₂pz)₃}₂]I₂, with a torsion angle of 8.7°, undergoes a spin crossover below 195 K, whereas the solvated crystalline form, [Fe{HC(3,5-Me₂pz)₃}₂]I₂·(CH₂Cl₂)₄, with the large torsion angle of 17.7°, does not undergo a spin crossover to the low-spin form above 4 K.^{6e}

Recent studies by Murray et al.^{7c} have also lead to conclusions similar to those outlined above for **1** that pyrazolyl ring twisting can have a significant impact on the spin-state crossover in these types of complexes. They have prepared and studied mixed ligand, tris(pyrazolyl)methane [FeLL']²⁺ complexes, most notably two polymorphs of [Fe{HC(3,5-Me₂(pz)₃}₂]{HC(pz)₃}(BF₄)₂. Careful analysis of the structures of the two polymorphs indicated the one that shows abrupt spin-crossover behavior (no phase change) needed a greater level of “molecular reorganization,” mainly associated with ring twisting, in going from one spin-state to the other than the form that showed a gradual spin-relaxation changeover.

The reasons for the small twist angle in complex **1**, in comparison with analogous complexes, must arise from intramolecular interligand interactions, crystal packing, as well as the size of the iron(II) ion. The other complex in Table 4 with a low average torsion angle, [Fe{HC(3,4,5-Me₃pz)₃}₂](BF₄)₂, is distinct from **1** in that this complex shows spin-state crossover at about 110 K, but this crossover is associated with a phase transition. As above, phase changes dominate the spin crossover, if present.

Complex **1** also has the unusual feature that its Mössbauer spectra require longer times to obtain spectra at higher temperatures than at lower temperatures. The spectrum obtained at 295 K and shown in Figure 4 required 13 days to acquire whereas the 4.2 to 85 K spectra required just 1 to 2 h each. This longer time required at the higher temperatures

is related to the unusual thermal factors, that is, the U_{iso} values obtained at 150 and 294 K, and the associated recoil free fraction, f , given by $f = \exp(-k^2\langle x^2 \rangle) = \exp(-k^2 U_{\text{iso}})$, where $k = 7.31 \times 10^{10} \text{ m}^{-1}$, is the wavevector of the 14.4 keV iron-57 Mössbauer-effect γ -ray. A plot of the U_{iso} and the associated f -factors¹⁷ for both **1** and $[\text{Fe}\{\text{HC}(3,5\text{-Me}_2\text{pz})_3\}_2(\text{BF}_4)_2]$ is shown in Supporting Information, Figure S1, a figure that reveals the dramatic differences in the thermal factors associated with the iron(II) sites in the two complexes.

The calculated f -factor of 0.170 obtained for **1** at 150 K corresponds predominately to the low-spin iron(II) state, whereas the calculated f -factor of 0.055 obtained at 294 K corresponds to an admixture of the low-spin and high-spin states. Because the high-spin f -factor is expected to be smaller than the low-spin f -factor, at 294 K the high-spin and low-spin f -factors may be estimated to be smaller and larger than 0.055, respectively. Hence, the high-spin fractions, p , given in Table 3B, and plotted in Figures 3b and 6 as the green points, fractions that have been obtained by assuming equal f -factors for the high-spin and low-spin fractions, must be adjusted for the different f -factors. If the 294 K high-spin f -factor is assumed to be 0.042, then the effective high-spin fraction is 82%, a value in excellent agreement with the percentage obtained from the magnetic measurements and shown as the black points in Figure 3b. Thus, the difference between the high-spin percentages obtained from the magnetic measurements and from the Mössbauer spectral measurements, a difference that is exemplified in Figure 3b by the black and green points, can be understood on the basis of both the temperature dependence of the total f -factor and the varying contributions of the different high-spin and low-spin f -factors.

Conclusions

A combination of X-ray structural, magnetic, and Mössbauer spectral studies have shown that **1** undergoes a gradual change from the low-spin form below 85 K to the high-spin form above 400 K. The Mössbauer results show that over this temperature range the complex is undergoing electronic spin-state relaxation between the two forms on the

Mössbauer time scale. The solid state structures show that **1** does *not* undergo a phase transition between 150 and 294 K. In our previous work with both poly(pyrazolyl)borate and poly(pyrazolyl)methane complexes of this type, we have shown that the phase change, if present, dominates the spin change generally leading to the observation of strongly cooperative spin changes over a small temperature range, frequently with hysteresis.^{5,6} Importantly, the structure at 294 K, a temperature where the cation is mainly in the high-spin form, shows that the twisting of the pyrazolyl-rings, a distortion observed when these ligands bond large metals, is unusually low in **1** for a high-spin iron(II) complex. This twisting issue is important to the spin-state change; in all cases the low-spin forms have low twisting angles because of the smaller size of low-spin iron(II). The combination of the lack of a phase change and the similarity of the twisting angles in the low- and high-spin forms allows the cations to gradually change from one form to the other. No cooperative spin-crossover or phase transition are needed for **1** to achieve the low-spin coordination environment with its substantially shorter Fe–N bond distances and lower twist angles. Rather, **1** can undergo a gradual spin-state transition from essentially the high-spin iron(II) state at 400 K to the low-spin iron(II) state at and below about 85 K.

Acknowledgment. The authors thank Dr. M. T. Sougrati for his help in obtaining some of the Mössbauer spectra. The authors acknowledge with thanks the financial support of the U.S. National Science Foundation through Grant CHE-0715559 (D.L.R.) and the Fonds National de la Recherche Scientifique, Belgium, through Grants 9.456595 and 1.5.064.05 (F.G.).

Supporting Information Available: The temperature dependence of the thermal factor and equivalent recoil-free fraction, temperature dependence of χ_M and μ_{eff} , and temperature dependence of the percentage of high-spin iron(II) at different assumed values of low-spin and high-spin μ_{eff} values. X-ray crystallographic files in CIF format for the structural determinations of **1**. This material is available free of charge via the Internet at <http://pubs.acs.org>.